



Deposited via The University of York.

White Rose Research Online URL for this paper:

<https://eprints.whiterose.ac.uk/id/eprint/234923/>

Version: Published Version

Article:

Johnson, Callum, Leslie, Kathryn, Franco Ortega, Sara et al. (2025) Identifying pathoadaptation in *Pseudomonas aeruginosa* using glycopolymer arrays. ACS sensors. ISSN: 2379-3694

<https://doi.org/10.1021/acssensors.5c03694>

Reuse

This article is distributed under the terms of the Creative Commons Attribution (CC BY) licence. This licence allows you to distribute, remix, tweak, and build upon the work, even commercially, as long as you credit the authors for the original work. More information and the full terms of the licence here:

<https://creativecommons.org/licenses/>

Takedown

If you consider content in White Rose Research Online to be in breach of UK law, please notify us by emailing eprints@whiterose.ac.uk including the URL of the record and the reason for the withdrawal request.

Identifying Pathoadaptation in *Pseudomonas aeruginosa* Using Glycopolymer Sensor Arrays

Callum Johnson, Kathryn G. Leslie, Sara Franco Ortega, James W. B. Moir, John M. Girkin, Helle Krogh Johansen, Ville-Petri Friman, and Clare S. Mahon*



Cite This: <https://doi.org/10.1021/acssensors.5c03694>



Read Online

ACCESS |



Metrics & More



Article Recommendations

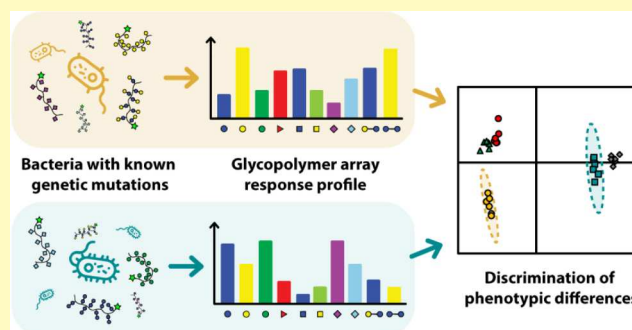


Supporting Information

ABSTRACT: In-host bacterial evolution presents a major barrier to effective infection management, driving phenotypic adaptations such as antibiotic resistance and altered virulence. *Pseudomonas aeruginosa*, a key opportunistic pathogen, frequently undergoes rapid evolutionary changes during chronic lung infections, complicating diagnosis and treatment. Current strain typing via whole genome sequencing or selective culturing is costly and time-intensive, and the complex relationship between genetic variations and the resulting phenotype makes clinically relevant pathotypes difficult to identify. Here, we report a cross-reactive, glycopolymer-based fluorescent sensor array capable of directly identifying phenotypic changes related to in-host evolution in *P. aeruginosa*.

The sensor array can accurately distinguish phenotypic variations arising from single-gene defects and discriminate clinical isolates with known differences in their evolutionary and pathoadaptive trajectories. Notably, our system is also capable of identifying *P. aeruginosa* isolates as distinct from other bacterial species commonly found in complex polymicrobial lung infections. Our modular platform presents an opportunity to develop sensor arrays that target carbohydrate recognition in a variety of pathogens, offering potential application as a rapid diagnostic tool to inform clinical treatment decisions based on the direct classification of phenotypic profiles.

KEYWORDS: sensor arrays, differential sensing, glycopolymers, biosensing, bacterial evolution, pathoadaptation, bacterial virulence



Chronic bacterial infections present huge societal challenges, reducing patient quality of life and placing significant pressures on healthcare systems.¹ In these cases, bacteria evade the initial response of the host and remain present for extended periods of time—in some cases through asymptomatic infections that may contribute to the dissemination of disease and may be subsequently reactivated within the host or through clinically apparent symptomatic infection.² During these prolonged infections, bacteria may evolve within the host,³ leading to persistent infections that are difficult to eradicate or manage. This process of “pathoadaptation” leads to genotypic and phenotypic changes in bacteria, such as altered protein expression, gain or loss of virulence traits, or resistance to antimicrobials, which is forecasted to contribute to 8.2 million annual global deaths by 2050.⁴

Pseudomonas aeruginosa is typically associated with chronic respiratory infections in people with cystic fibrosis (pwCF), an autosomal recessive disorder affecting over 160 000 people worldwide,⁵ where deficiencies in the innate immune response lead to extreme vulnerability to lung infections, which severely limit life expectancy (the median age at death of pwCF who died in 2018 was 31 years).⁶ Hospital-acquired *P. aeruginosa* infections are also a frequent cause of mortality for patients

undergoing mechanical ventilation.⁷ Initially, *P. aeruginosa* typically displays a nonmucoid phenotype⁸ but rapidly evolves to chronic infective pathotypes characterized by the formation of mucoid alginate biofilms, production of adhesins, antibiotic resistance, and characteristic “loss of function” mutations, including loss of the O-antigen.⁹ These pathotypes are much more difficult to eradicate with antibiotics,¹⁰ leading to persistent, life-limiting infections.

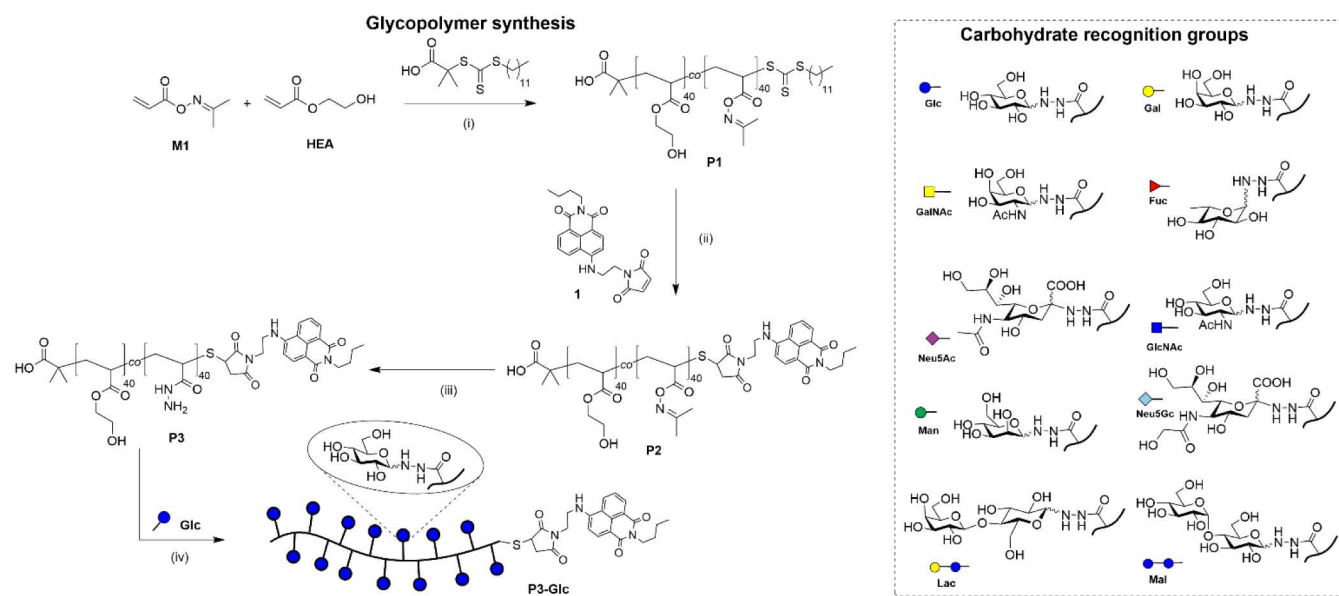
Current strain-typing protocols are costly and time-intensive, relying on selective culturing methods¹¹ or whole genome sequencing.¹² While diversification within hosts is driven by genetic changes and subsequent selection,^{13,14} the link between genetic variation and the display of functionally different pathotypes is not always clear. A recent longitudinal study focusing on *P. aeruginosa* evolution within immunocompromised patients’ lungs found that different genetic mutations

Received: October 6, 2025

Revised: November 14, 2025

Accepted: November 19, 2025

Scheme 1. Glycopolymer Synthesis and Carbohydrate Recognition Groups: (i) AIBN, 1,4-Dioxane, 70 °C, 2.5 h; (ii) 1, Hexylamine, Et₃N, TCEP, DMF, rt, 18 h; (iii) N₂H₄·H₂O, DMF, 0 °C, 1 h; and (iv) 100 mM NaOAc, Aniline, pH 5.5, 50 °C, 18 h



can lead to the same pathoadaptation at the phenotypic level,¹⁵ making it difficult to predict pathotypes based solely on genetic characteristics. A potential explanation for this observation is that nearly 10% of the *P. aeruginosa* genome encodes regulatory proteins,¹⁶ providing scope for large phenotypic differences arising from small but significant genetic changes. Therefore, the direct classification of evolving pathogen genotypes based on their virulence characteristics or other phenotypic properties could offer a more robust strategy for rapid diagnostics and efficient treatment compared with genomic information alone.

Many key events in the initiation and progression of bacterial infections are underpinned by molecular recognition at surfaces,¹⁷ including the attachment of bacteria to cellular surfaces and their adhesion within biofilms.¹⁸ *P. aeruginosa*, like many other bacteria, produces lectins that interact with carbohydrate motifs displayed on epithelial surfaces and within exopolysaccharide matrices produced during biofilm formation. Several studies have highlighted variation in cellular glycosylation patterns within pwCF, with the predominant display of an asialylated derivative (aGM1) of the mammalian glycolipid GM1 on the epithelial surface, resulting in increased levels of fucose and decreased quantities of neuraminic acid.^{19–21} This variation has been associated with differences in the ability of *P. aeruginosa* to attach to epithelial surfaces via adhesins, a crucial stage in the initial process of colonization. In established infections, cellular surface recognition is likely to be less important than attachment within the biofilm matrix, as suggested by the frequent loss of lectin-bearing pili and flagella within adapted pathotypes.²²

While the importance of lectins in the establishment and progression of bacterial infection renders them attractive targets for the design of sensors and diagnostics, the development of specific recognition motifs for lectins is complicated by their typically low binding affinities for complementary carbohydrates and their promiscuity in carbohydrate recognition.¹⁷ The avidity of interactions can be enhanced through the cluster glycoside effect, by attaching

multiple copies of the carbohydrate motif to a macromolecular scaffold.^{17,23,24} The cross-reactivity in carbohydrate recognition presents an opportunity to employ array-based sensing methods^{25–29} for the identification of analytes. An array-based approach has been used to screen phenotypic changes in *Staphylococcus aureus* and *Escherichia coli* after exposure to antibiotics.³⁰ We recently demonstrated that arrays of fluorescent glycopolymers can discriminate lectins and a selection of pathogenic bacteria through differences in carbohydrate recognition behaviour,²⁴ encompassing a broad range of bacteria including *Salmonella enterica*, *Escherichia coli*, vancomycin-sensitive and -resistant strains of *Enterococcus faecium* and *P. aeruginosa* strains PAO1 and PA14. The extension of sensing capability from isolated lectins to bacteria was expected, on account of the prevalence of lectins on bacterial surfaces, and the importance of carbohydrate recognition during infection.¹⁷ The discrimination of PAO1 and PA14 strains, representing *P. aeruginosa* of moderate and severe virulence, however, was notable, and we decided to explore the discrimination of *P. aeruginosa* isolates of different virulence behaviors, with a view to developing a clinical tool to identify problematic phenotypic changes over the course of prolonged infections.

Here, we describe the synthesis and optimization of a fluorescent glycopolymer sensor array that can discriminate *P. aeruginosa* transposon insertion mutants that differ in their virulence profiles due to mutations in genes associated with several pathoadaptations. We also extend the discriminatory power of the sensor array to differentiate a selection of clinical *P. aeruginosa* CF-lung isolates representing different evolutionary pathoadaptive trajectories, and to discriminate a subset of *P. aeruginosa* CF-lung isolates from other common lung pathogens frequently presented in polymicrobial infections of the CF lung.

RESULTS AND DISCUSSION

The glycopolymers within our sensor array were constructed on a conserved polymer backbone, P1, accessed via the

reversible addition-fragmentation chain transfer (RAFT) polymerization of 2-hydroxyethyl acrylate (HEA) and **M1**, an acrylate derivative bearing an oxime functionality (Scheme 1). **P1** displayed a total degree of polymerization of 80, comprising HEA and **M1** in an approximately 1:1 ratio. Kinetic analysis of the polymerization (ESI Section 1.2) demonstrated that both monomers were incorporated at an approximately equal rate, leading to a random copolymer. The ω -trithiocarbonate unit was subjected to aminolysis to generate a thiol, which was immediately reacted with a maleimide-functionalized 4-amino-1,8-naphthalimide, **1**, to generate a fluorescent polymer scaffold, **P2**. The oxime units were then treated with hydrazine hydrate to yield a polymer with pendant acylhydrazide functionalities (**P3**), which were used to install multiple copies of one of ten reducing sugars, generating an array of glycopolymers expected to interact to varying extents with *P. aeruginosa* surface determinants.

We first chose to investigate the ability of the sensor array to discriminate a selection of engineered *P. aeruginosa* transposon insertion mutants *in vitro*, with known genetic differences in selected pathoadaptive genes (Table 1). From a library of

transposon-insertion mutant strains maintained by Held et al.,³¹ we selected a subset of mutants that display defects in genes associated with virulence: lectin production (PA2570, Δ lecA), alginate biosynthesis (PA3542, Δ alg44), regulatory protein expression (PA4856, Δ retS), and twitching motility (PA4959, Δ fimX), as well as PAO1,¹⁶ representing the complete genome prior to transposon-insertion mutation. Full experimental procedures for the assessment of array response to bacterial addition are available in the ESI (Section 2.1). Briefly, bacteria were grown to saturation (stationary phase) from glycerol stocks in nutrient-rich medium, and then cells were isolated by centrifugation and resuspended in an equivalent volume of phosphate-buffered saline (PBS) at pH 7.4.

Emission spectra were recorded for each receptor within the array (5.0 μ M, PBS pH 7.4, 6 replicates), before and after the addition of bacterial suspensions (10 μ L aliquot). The integrated emission intensity was used to calculate relative changes in fluorescence emission for each glycopolymer (I/I_0). The effect of dilution was accounted for by adding an equivalent volume of buffer to each receptor in the array and dividing receptor I/I_0 values by the mean change in the emission intensity for each receptor upon dilution. Upon addition of bacteria to glycopolymers, increases in emission intensity of up to 2-fold were observed with no significant change in emission maximum (Figure 1A,B). 4-Amino-1,8-naphthalimides are highly sensitive to the polarity of their surrounding microenvironment,^{37,38} with enhanced emission in nonpolar media. We propose that upon the binding of glycopolymers to the bacterial surface, the naphthalimide unit resides in a less polar environment than the surrounding aqueous medium, leading to increased emission intensity.

The resulting dataset was interrogated using linear discriminant analysis (LDA),³⁹ a multivariate statistical tool that analyzes the variance within the dataset and constructs a

Table 1. *P. aeruginosa* Genes and Associated Functions

Gene	Associated pathway	Function	Ref(s)
<i>lecA</i>	LecA production	LecA is involved in adhesion to host cells via galactose-terminated glycans	32
<i>fimX</i>	Twitching motility	Regulation of twitching motility in response to environmental cues	33
<i>alg44</i>	Alginate biosynthesis	Alginate is a structurally important polysaccharide in biofilms	34
<i>retS</i>	Regulatory protein expression	Modulates phage resistance, biofilm formation, and type IV pili function	35,36

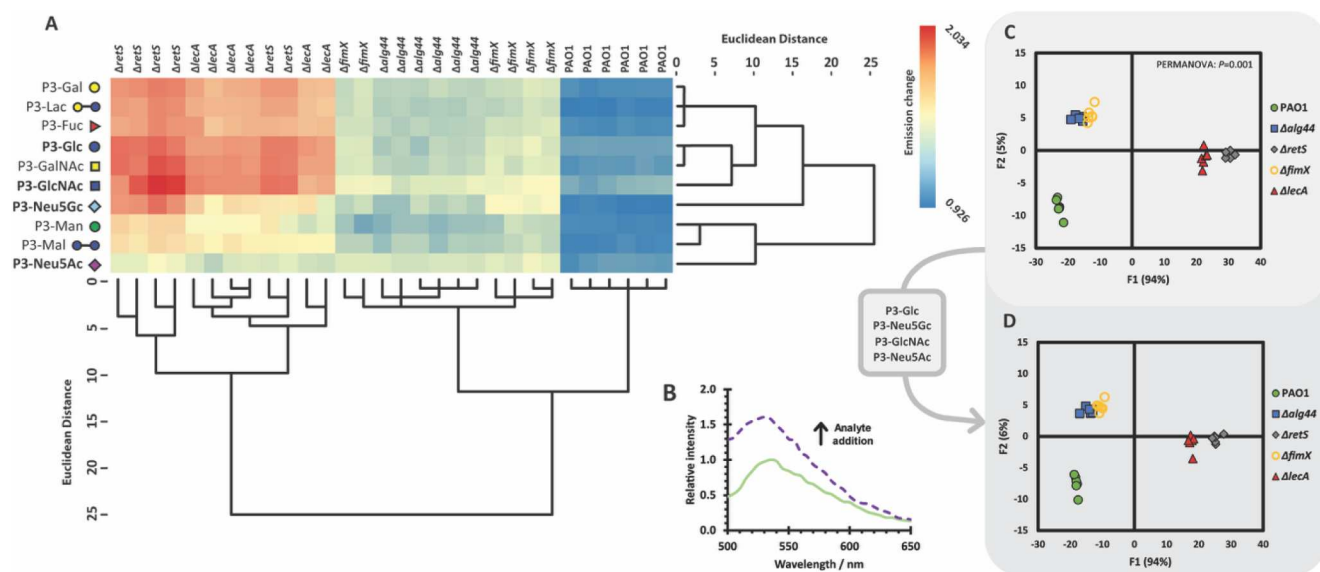


Figure 1. (A) Heat map of fluorescence emission changes for each glycopolymer and bacterial replicate, with dendrograms produced through hierarchical cluster analysis (HCA) of glycopolymer responses to transposon mutants. (B) Representative example of a change in fluorescence emission intensity ($\lambda_{\text{ex}} = 450$ nm) upon addition of mutant Δ retS to P3-GlcNAc. (C) Canonical LDA score plot for the analysis of transposon mutants performed in sextuplicate (5.0 μ M receptors, pH 7.4). (D) Canonical LDA score plot for the analysis of transposon mutants performed in sextuplicate (5.0 μ M receptors, pH 7.4) with a simplified array of glycopolymers, consisting of P3-Glc, P3-GlcNAc, P3-Neu5Ac, and P3-Neu5Gc. 100% of original grouped cases were correctly classified, and 100% of cross-validated grouped cases were correctly classified.

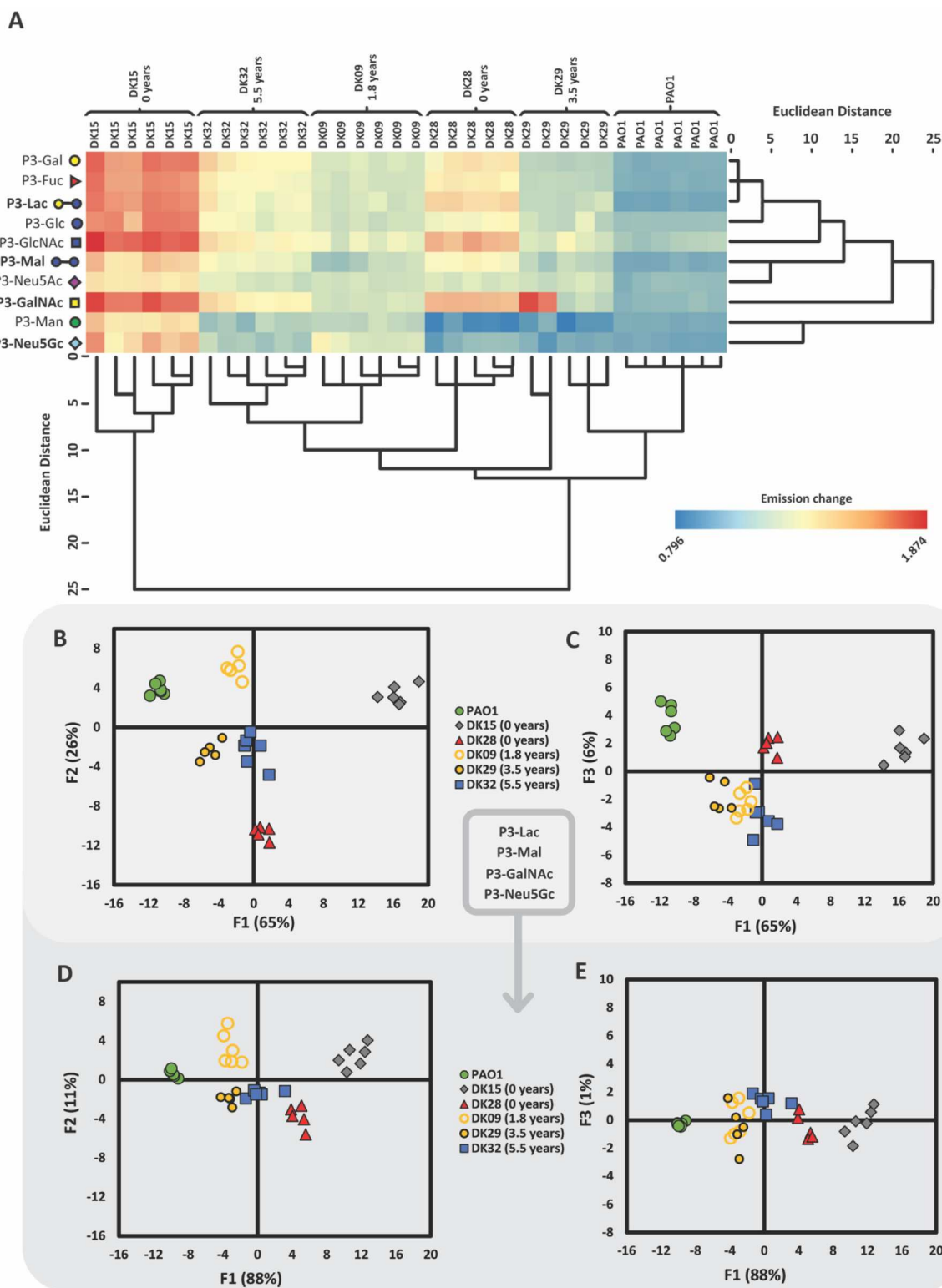


Figure 2. (A) Heat map of fluorescence emission changes for each glycopolymer and replicate with dendrograms produced through hierarchical cluster analysis (HCA) of glycopolymer responses to *Pseudomonas aeruginosa* clinical CF-lung isolates. (B) Canonical LDA score plots for functions 1 & 2 and (C) functions 1 & 3 for the analysis of clinical isolates of known evolutionary lineage performed in sextuplicate ($5.0 \mu\text{M}$ receptors, pH 7.4). 100% of original grouped cases were correctly classified and 94% of cross-validated grouped cases were correctly classified. (D) Canonical LDA score plots for functions 1 & 2, and (E) functions 1 & 3 for the analysis of clinical isolates of known evolutionary lineage performed in sextuplicate ($5.0 \mu\text{M}$ receptors, pH 7.4) with a simplified array of glycopolymers, consisting of P3-Lac, P3-Mal, P3-GalNAc, and P3-Neu5Gc. 100% of original grouped cases were correctly classified, and 97% of cross-validated grouped cases were correctly classified.

model that categorizes data points using a combination of linear discriminant functions that describe the responses of the

glycopolymers to each analyte. The resulting algorithm can be used to assign unknown analytes to one of these categories.

LDA enabled effective discrimination of the mutants, as shown graphically (Figure 1C), with 100% of the variance accounted for by the first and second linear discriminant functions. This analysis enabled classification of the mutants with 100% accuracy. The variance between each pair of clusters identified by LDA was demonstrated to be of statistical significance by PERMANOVA⁴⁰ (Adonis2) (ESI Table S6). The predictive power of the model was confirmed using a “leave-one-out” validation procedure, whereby each data point is systematically excluded from the training set, and the linear discriminant functions calculated using the rest of the data are used to determine its identity. Mutants were identified with a high degree of accuracy (93%) with two discrepancies arising from mutual misclassification of the $\Delta fimX$ mutant to the $\Delta alg44$ mutant (ESI Table S7). To further evaluate the predictive ability of the sensor array, the data set was then divided into “training” (4 replicates per analyte) and “unknown” (2 replicates per analyte) datasets (ESI Section 2.7). The “training” dataset was used to construct an LDA algorithm, which was used to assign the “unknown” data points. The “unknown” analytes were assigned with 100% accuracy (Table S10).

To assess the ability of the sensor array to identify bacterial analytes at different effective concentrations, PAO1 was grown to saturation and resuspended in PBS at pH 7.4, as previously described, before these suspensions were further diluted by factors of 1 in 2 and 1 in 4 (ESI Section 2.9). These suspensions were exposed to glycopolymers within the sensor array, as previously described, and assigned as “unknown” analytes using the scoring algorithm established by LDA (Figure 1C, Table S5). In all cases, analytes were scored as PAO1 (Table S13, Figure S5).

To assess whether equivalent discrimination could be achieved using a smaller number of glycopolymers, hierarchical cluster analysis (HCA) was used to identify glycopolymers providing similar response profiles. HCA is a statistical clustering technique that groups data points in a stepwise process based on identifying dissimilarity within the dataset, represented graphically as a dendrogram (Figure 1A). The elimination of glycopolymers displaying similar response profiles allowed us to reduce the number of receptors required for discrimination to four glycopolymers: P3-Glc, P3-GlcNAc, P3-Neu5Ac, and P3-Neu5Gc. Subsequent LDA conducted with these four glycopolymers still enabled discrimination of the selected transposon mutants with 100% accuracy (Figure 1D). In a “leave-one-out” validation procedure, mutants were assigned to their groups with 100% accuracy (ESI Table S8), presenting an improvement in predictive performance compared to the complete array of 10 glycopolymers. The hold-out validation procedure described above was repeated, resulting in the assignment of “unknown” analytes with 100% accuracy. This increase in validation scores, while initially unexpected, may reflect that removing the effects of duplication in sensor responses simplifies the features within the dataset that can provide discrimination.⁴¹

Notably, neuraminic acid-decorated glycopolymers P3-Neu5Ac and P3-Neu5Gc contribute significantly to the discriminatory power of the sensor array, as indicated by HCA (Figure 1) and PCA loading plots (Figure S4). This observation may reflect the importance of neuraminic acids in cellular recognition,⁴² accounting for a large proportion of the mammalian glycocalyx, with implications for numerous processes of microbial pathogenesis. Alternatively, this

behavior may arise as a consequence of the inherent features of the neuraminic acid glycopolymers. Conjugation efficiencies for Neu5Ac and Neu5Gc were noted to be lower than those for other carbohydrates, resulting in their presence in lower proportions on the polymer backbone (Table S2). This feature may present opportunities for discrimination arising from complementary, less-specific interactions, such as electrostatic effects, in addition to protein–carbohydrate recognition. P3-Neu5Ac and P3-Neu5Gc are additionally distinct from other glycopolymers in the sensor array in that they are multiply negatively charged, and this difference in electrostatics is likely to amplify the increase in the emission of the naphthalimide probe upon recognition of cell-surface proteins, as the net change in polarity of the medium surrounding the fluorophore upon binding will be greater.³⁷

Analytes discriminated by the sensor array display limited genetic differences from one another. Each transposon mutant differs from the reference PAO1 strain by ISlacZ/hah or ISphoA/hah transposon insertion³¹ in a single gene, disrupting the open reading frames corresponding to the production of a protein associated with a virulence factor or signaling pathway. The effective discrimination of mutants that are genetically similar, yet display different virulence traits, suggests that glycopolymer sensing arrays could find utility in identifying pathoadaptive traits in clinical isolates of *P. aeruginosa* obtained directly from pwCF.¹⁶

From a library of clinical *P. aeruginosa* isolates obtained during a long-term study on pwCF by Johansen et al.,⁴³ we chose five genetically distinct clinical isolates belonging to different “DK” lineages (Pa80 representing DK09, Pa427 representing DK15, Pa202 representing DK28, Pa209 representing DK29, Pa247 representing DK32). These isolates represent different stages of pathoadaptation according to the duration of the infection (0–5.5 years) and are known to display significant genetic and phenotypic differences, having independent evolutionary histories within different patients, and having previously been categorized into distinct genotypes.⁴³ The isolate representing the genotype DK09 was identified as having a recent mutation in the *retS* gene, unique among the clinical isolates we tested, which encodes a regulatory protein we previously identified as a key driver of phenotypic changes.⁴³ *pilQ*, a gene responsible for transmembrane passage of type IV pili via the PilQ secretin, had undergone mutation in the DK15 and DK32 samples.⁴⁴ Changes to the surface composition of type IV pili may alter glycan-binding properties by affecting the interactions of pili-associated lectins.

Isolates were cultured in nutrient-rich medium and exposed to glycopolymers as detailed previously, resulting in changes to the emission intensity of the naphthalimide probe (Figure 2A), with quenching of emission observed in some cases, in addition to increases in emission intensity, as observed previously. LDA of the changes in emission of the glycopolymers upon exposure to the isolates enabled effective discrimination of the isolates with 100% accuracy, as shown graphically (Figure 2B,C). In this case, 91% of variance within the dataset could be explained by a combination of the first two linear discriminant functions, F1 and F2, accounting for 65% and 26% of variance, respectively (Figure 2B). There was also a non-insignificant contribution to the variance arising from a third function, F3 (6%) (Figure 2C). In a leave-one-out validation assessment, the bacteria were classified with 100% accuracy (ESI Table S19). When the data was split into

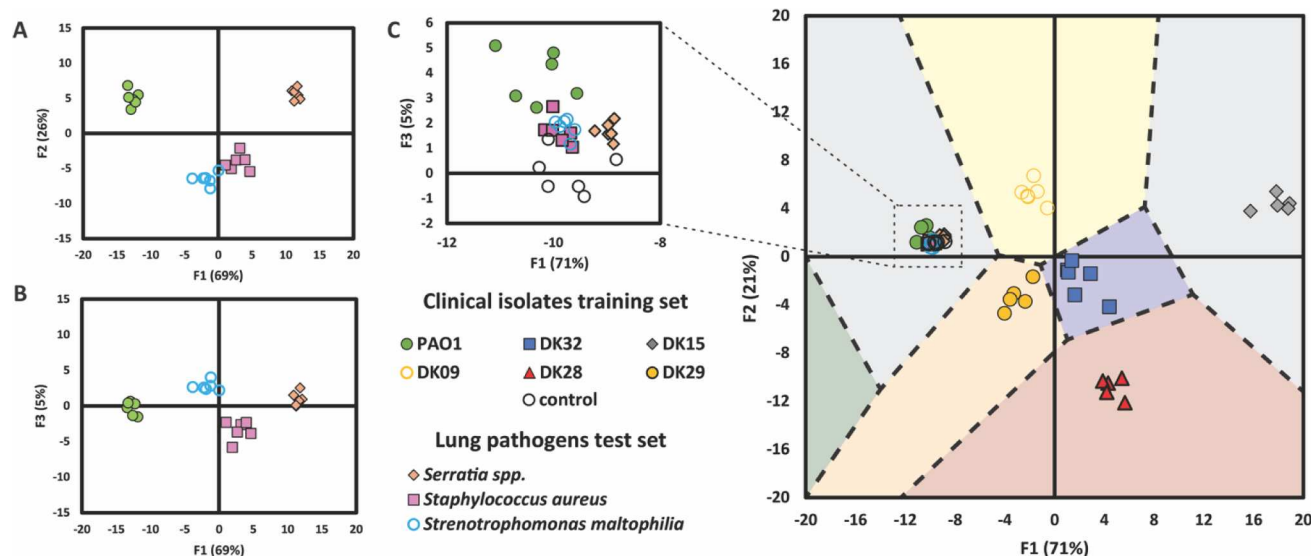


Figure 3. (A) Canonical LDA score plots for functions 1 & 2 and (B) functions 1 & 3 for the analysis of lung pathogens performed in sextuplicate ($5.0 \mu\text{M}$ receptors, pH 7.4). 100% of original grouped cases were correctly classified with 96% of cross-validated grouped cases correctly classified. (C) Territorial map with LDA scores for *P. aeruginosa* CF-lung isolates, including a control and several lung pathogens (*Serratia* spp., *Staphylococcus aureus*, and *Stenotrophomonas maltophilia*), unknown to the LDA model ($5.0 \mu\text{M}$ receptors, pH 7.4). A partial 3D plot showing the third scoring function, F3, is supplied in the ESI (Figure S9).

“training” and “unknown” datasets and assessed as previously described (ESI Section 3.7), the “unknown” analytes were assigned with 90% accuracy, with a single misclassification of a DK32 analyte to DK28 (Table S22). The scoring algorithm established via LDA of this dataset (Figure 2, Table S17) was used to assign diluted suspensions of PAO1, prepared as described earlier. In all cases, analytes were scored as PAO1 (Table S25, Figure S8). Evolution toward decreased virulence but increased drug resistance has been shown to take place during the course of *P. aeruginosa* infection, most significantly during the initial 2–3 years of infection.^{15,43} In LDA analysis, strains sampled earliest in their infection (corresponding with genotypes DK15 and DK28, sampled at first appearance within patient) were more clearly separated from more established strains, which were grouped more closely together (corresponding to DK09, DK29, and DK32 sampled at 1.8, 3.5, and 5.5 years after the first detection of the genotype, respectively). This observation may be consistent with a changing phenotype over time that becomes harder to differentiate as the different bacterial genotypes converge, a hypothesis we intend to examine in detail in a future study. HCA (Figure 2A) and PCA (Figure S7) were again used to find combinations of glycopolymers with similar response profiles, with the aim of reducing the number of sensors required to provide effective discrimination. Again, this analysis enabled the simplification of the array to just four glycopolymers: P3-Lac, P3-Mal, P3-GalNAc, and P3-Neu5Gc. Subsequent LDA conducted with these glycopolymers enabled discrimination of the selected isolates with 100% accuracy (Figure 2D,E). Again, utilizing a “leave-one-out” validation procedure, isolates were assigned to their groups with 97% accuracy, with a single discrepancy arising from misclassification of DK32 as DK28 (Table S20). The glycopolymers identified as core to driving discrimination were not entirely identical to those identified as key to discrimination of transposon mutants, although some recognition elements are conserved. Interestingly, of the two neuraminic acid functionalized glycopolymers included within

the complete array, P3-Neu5Gc was demonstrated to contribute more to discrimination than P3-Neu5Ac. *N*-acetylneuraminic acid (Neu5Ac) is displayed on human cell surfaces and is known to play a key role as a cellular recognition element and in the evasion of host immune mechanisms, while *N*-glycolylneuraminic acid (Neu5Gc) is an analogue which is displayed on cell surfaces of other mammalian cells.⁴² Within pwCF, however, epithelial display of Neu5Ac is reduced as a consequence of display of the asialylated GM1 derivative aGM1.¹⁹ Moreover, in persistent lung infections, the environment immediately surrounding a bacterium is likely to be dominated by the biofilm: bacteria are primarily exposed to exopolysaccharides and other bacteria, rather than the mammalian epithelial surface itself. P3-Lac and P3-Mal present terminal galactose and glucose units, respectively, which are displayed within *P. aeruginosa* exopolysaccharide.⁴⁵

The ability to rapidly discriminate *P. aeruginosa* strains of different, clinically relevant evolutionary lineages would present a major advantage for the monitoring of persistent infections, enabling improved clinical decision-making. *P. aeruginosa* infections within immunocompromised patients, however, are typically a single component of a complex, multispecies infection,^{46,47} although *P. aeruginosa* is generally considered to be responsible for the majority of irreversible lung tissue damage.⁴⁸ We therefore assessed the ability of the array to identify *P. aeruginosa* pathotypes among a selection of other bacteria typically present within the CF lung: *Staphylococcus aureus*, *Serratia* spp., and *Stenotrophomonas maltophilia*. *S. aureus* is a Gram-positive bacterial pathogen, which is frequently implicated in polymicrobial respiratory infections in pwCF.⁴⁹ *S. maltophilia* is also commonly coidentified in pwCF colonized with *P. aeruginosa*^{50,51} and may transition to a similar mucoid phenotype to that displayed by *P. aeruginosa*. *S. maltophilia* isolates have been misidentified as *Pseudomonas*,⁵² with selective culturing methods or metabolic studies developed to enable identification.¹¹ *Serratia* spp. is a Gram-

negative bacterium which is increasingly implicated in hospital-acquired infections, including respiratory infections in immunocompromised patients.⁵⁵

The ability of the sensor array to discriminate these lung pathogens was first established by comparing the array's response to *S. aureus*, *S. maltophilia*, *Serratia*, and PAO1 as a representative *P. aeruginosa* isolate. Using the same experimental procedure as previously employed, lung pathogens were grown in nutrient-rich medium before resuspension in an equivalent amount of buffer. Glycopolymers within the array (5.0 μM , 6 replicates) were then exposed to the bacteria (10 μL aliquots), and LDA of the changes in emission of the probes upon exposure to the isolates (I/I_0) enabled effective discrimination of each genus with 100% accuracy (Figure 3A,B). "Leave-one-out" cross-validation showed classification of each species with 92% accuracy, with two mutual misclassifications of *S. maltophilia* and *S. aureus* (ESI Table S31). Data were subsequently split into "training" and "unknown" datasets and assessed as previously described (ESI Section 4.6). In this case, the "unknown" analytes were assigned with 88% accuracy, with a single misclassification of *S. aureus* to *S. maltophilia* (Table S33). The discriminatory power of the sensor array at varying effective concentrations of analytes was again probed using "unknown" analytes consisting of PAO1 grown to saturation, resuspended in PBS, and diluted by factors of 1 in 2 and 1 in 4 as previously described. Upon scoring with the algorithm generated by LDA (Figure 3A,B; Table S29), these analytes were identified as *S. maltophilia* (Table S35), highlighting a limitation of the array in identifying analytes at varying effective concentrations. This difficulty likely arises because the changes in naphthalimide emission observed upon exposure to the range of pathogens are smaller than those observed upon exposure to *P. aeruginosa* analytes, rendering pattern recognition more challenging. This difference in response reflects the design principles of our sensor array: to best enable discrimination of *P. aeruginosa*-strains we have focused on incorporating carbohydrate-protein interactions that are important within the evolutionary trajectory of this pathogen. In order to improve the sensor array's ability to discriminate different respiratory pathogens at different effective concentrations, the receptor pool should be widened to encompass other respiratory disease-relevant processes of molecular recognition to elicit a greater response upon exposure to analytes.

To explore the predictive power of the glycopolymer sensor array in identifying *P. aeruginosa* isolates as distinct from other lung pathogens, a training dataset was constructed using the response of the complete array to the *P. aeruginosa* clinical isolates tested above (DK09, DK15, DK28, DK29, DK32), PAO1, and a "control" sample consisting of an aliquot of PBS buffer. LDA analysis of this dataset was used to construct a scoring algorithm, which was used to assign the lung pathogen analytes to the most relevant category. The three lung pathogens were all subsequently classified within the "control" group (18/18), with score functions located within the boundaries of this category (Figure 3C; Figure S9). This analysis demonstrates that the glycopolymer sensor array can identify a bacterial infection as either *P. aeruginosa* or an alternative pathogen, in addition to enabling the discrimination of common CF lung pathogens and of *P. aeruginosa* mutants.

CONCLUSIONS

We have described a glycopolymer sensor array comprising a conserved polymer scaffold, 10 carbohydrate recognition motifs, and a fluorescent reporting group, which can identify phenotypic variation in virulence profiles within *P. aeruginosa*, an opportunistic pathogen associated with persistent respiratory infections in immunocompromised patients. The sensor array can identify transposon-insertion mutants with differences in genes associated with pathoadaptive traits, including adhesin production, alginate biosynthesis, and motility. The sensor array was also demonstrated to classify clinical isolates of *P. aeruginosa* representing different evolutionary lineages, displaying different degrees of pathoadaptation and virulence traits. Through detailed statistical analysis of the array's response, the number of sensors required to achieve effective discrimination can be reduced to just four, streamlining the process of identification and presenting a route to multiplexed combinations of sensors.

Our sensor array was also shown to be capable of identifying *P. aeruginosa* isolates as distinct from other, similar bacteria commonly associated with persistent infections in pwCF—an important distinction considering that *P. aeruginosa* is thought to be responsible for the majority of irreversible tissue damage in polymicrobial infections.⁴⁸ This system could provide the underpinning technology for the development of diagnostic platforms to discriminate *P. aeruginosa* pathotypes and identify virulence features within complex polymicrobial infections, informing treatment decisions. Moreover, given the ubiquity of carbohydrate recognition processes within many key processes of disease, our modular design presents a route to the development of glycopolymer sensor arrays for a host of other bacterial or viral pathogens.

ASSOCIATED CONTENT

Data Availability Statement

Polymer characterization data, raw spectroscopic input data and statistical models may be downloaded at <http://doi.org/10.15128/r1mp48sc83w>.

Supporting Information

The Supporting Information is available free of charge at <https://pubs.acs.org/doi/10.1021/acssensors.5c03694>.

Synthetic details, characterization, raw data, statistical analysis (PDF)

AUTHOR INFORMATION

Corresponding Author

Clare S. Mahon — Department of Chemistry, Durham University, Durham DH1 3LE, U.K.; orcid.org/0000-0002-7358-1497; Email: clare.mahon@durham.ac.uk

Authors

Callum Johnson — Department of Chemistry, Durham University, Durham DH1 3LE, U.K.

Kathryn G. Leslie — Department of Chemistry, Durham University, Durham DH1 3LE, U.K.; orcid.org/0000-0002-6816-2845

Sara Franco Ortega — Department of Biology, University of York, York YO10 SDD, U.K.; orcid.org/0000-0001-8924-464X

James W. B. Moir — Department of Biology, University of York, York YO10 SDD, U.K.; orcid.org/0000-0003-2972-5235

John M. Girkin – Department of Physics, Durham University, Durham DH1 3LE, U.K.; orcid.org/0000-0003-2568-3576

Helle Krogh Johansen – Department of Clinical Microbiology 9301, Copenhagen University Hospital, Ringhospitalet, Copenhagen 2100, Denmark; Department of Clinical Medicine, Faculty of Health and Medical Sciences, University of Copenhagen, Copenhagen N 2200, Denmark

Ville-Petri Friman – Department of Biology, University of York, York YO10 5DD, U.K.; Department of Microbiology, Faculty of Agriculture and Forestry and Viikki Biocenter, University of Helsinki, Helsinki FI-00014, Finland

Complete contact information is available at:

<https://pubs.acs.org/10.1021/acssensors.5c03694>

Author Contributions

The manuscript was written through the contributions from all authors. All authors have given their approval to the final version of the manuscript.

Funding

This work was supported by the Engineering and Physical Sciences Research Council (EP/X014479/1; UKRI Future Leaders Fellowship MR/V027018; MoSMED CDT EP/S022791/1). H.K.J. was supported by a Challenge Grant (NNF19OC0056411) and a clinical research stipend (NNF12OC1015920) from the Novo Nordisk Foundation.

Notes

The authors declare no competing financial interest.

ACKNOWLEDGMENTS

We are grateful for the financial support from the Cystic Fibrosis Foundation (Grant SINGH24R0), which maintains the PAO1 mutant collection. The authors thank Dr. Juan A. Aguilar of the NMR service and Peter Stokes of the mass spectrometry service at Durham University for assistance with experiments.

REFERENCES

- (1) European Centre for Disease Prevention and Control *Assessing the health burden of infections with antibiotic-resistant bacteria in the EU/EEA, 2016-2020*; European Centre for Disease Prevention and Control: Stockholm, 2022.
- (2) Grant, S. S.; Hung, D. T. Persistent bacterial infections, antibiotic tolerance, and the oxidative stress response. *Virulence* **2013**, *4* (4), 273–283.
- (3) Didelot, X.; Walker, A. S.; Peto, T. E.; Crook, D. W.; Wilson, D. J. Within-host evolution of bacterial pathogens. *Nat. Rev. Microbiol.* **2016**, *14* (3), 150–162.
- (4) Naghavi, M.; Vollset, S. E.; Ikuta, K. S.; Swetschinski, L. R.; Gray, A. P.; Wool, E. E.; Robles Aguilar, G.; Mestrovic, T.; Smith, G.; Han, C.; et al. Global burden of bacterial antimicrobial resistance 1990-2021: a systematic analysis with forecasts to 2050. *Lancet* **2024**, *404* (10459), 1199–1226.
- (5) Guo, J.; Garratt, A.; Hill, A. Worldwide rates of diagnosis and effective treatment for cystic fibrosis. *J. Cyst. Fibros.* **2022**, *21* (3), 456–462.
- (6) Marshall, B.; Faro, A.; Elbert, A.; Fink, A.; Sewall, A.; Loeffler, D.; Fernandez, G.; Ostrenga, J.; Petren, K.; Wu, R.; et al. *Cystic Fibrosis Foundation Patient Registry 2018 Annual Data Report*; Cystic Fibrosis Foundation, 2018.
- (7) Melsen, W. G.; Rovers, M. M.; Groenwold, R. H.; Bergmans, D. C.; Camus, C.; Bauer, T. T.; Hanisch, E. W.; Klarin, B.; Koeman, M.; Krueger, W. A.; et al. Attributable mortality of ventilator-associated pneumonia: a meta-analysis of individual patient data from

randomised prevention studies. *Lancet Infect. Dis.* **2013**, *13* (8), 665–671.

(8) Douglas, T. A.; Brennan, S.; Gard, S.; Berry, L.; Gangell, C.; Stick, S. M.; Clements, B. S.; Sly, P. D. Acquisition and eradication of *P. aeruginosa* in young children with cystic fibrosis. *Eur. Respir. J.* **2009**, *33* (2), 305.

(9) Breidenstein, E. B. M.; de la Fuente-Núñez, C.; Hancock, R. E. W. *Pseudomonas aeruginosa*: all roads lead to resistance. *Trends Microbiol.* **2011**, *19* (8), 419–426.

(10) Winstanley, C.; O'Brien, S.; Brockhurst, M. A. *Pseudomonas aeruginosa* Evolutionary Adaptation and Diversification in Cystic Fibrosis Chronic Lung Infections. *Trends Microbiol.* **2016**, *24* (5), 327–337.

(11) Brooke, J. S. *Stenotrophomonas maltophilia*: an Emerging Global Opportunistic Pathogen. *Clin. Microbiol. Rev.* **2012**, *25* (1), 2–41.

(12) Simar, S. R.; Hanson, B. M.; Arias, C. A. Techniques in bacterial strain typing: past, present, and future. *Curr. Opin. Infect. Dis.* **2021**, *34* (4), 339–345.

(13) Harris, S. R.; Robinson, C.; Steward, K. F.; Webb, K. S.; Paillot, R.; Parkhill, J.; Holden, M. T.; Waller, A. S. Genome specialization and decay of the stranglers pathogen, *Streptococcus equi*, is driven by persistent infection. *Genome Res.* **2015**, *25* (9), 1360–1371.

(14) Weinert, L. A.; Welch, J. J. Why might bacterial pathogens have small genomes? *Trends Ecol. Evol.* **2017**, *32* (12), 936–947.

(15) Bartell, J. A.; Sommer, L. M.; Haagensen, J. A. J.; Loch, A.; Espinosa, R.; Molin, S.; Johansen, H. K. Evolutionary highways to persistent bacterial infection. *Nat. Commun.* **2019**, *10* (1), 629.

(16) Stover, C. K.; Pham, X. Q.; Erwin, A. L.; Mizoguchi, S. D.; Warren, P.; Hickey, M. J.; Brinkman, F. S. L.; Hufnagle, W. O.; Kowalik, D. J.; Lagrou, M.; et al. Complete genome sequence of *Pseudomonas aeruginosa* PAO1, an opportunistic pathogen. *Nature* **2000**, *406* (6799), 959–964.

(17) Bernardi, A.; Jimenez-Barbero, J.; Casnati, A.; De Castro, C.; Darbre, T.; Fieschi, F.; Finne, J.; Funken, H.; Jaeger, K.-E.; Lahmann, M.; et al. Multivalent glycoconjugates as anti-pathogenic agents. *Chem. Soc. Rev.* **2013**, *42* (11), 4709–4727.

(18) Pizarro-Cerdá, J.; Cossart, P. Bacterial Adhesion and Entry into Host Cells. *Cell* **2006**, *124* (4), 715–727.

(19) Imundo, L.; Barasch, J.; Prince, A.; Al-Awqati, Q. Cystic fibrosis epithelial cells have a receptor for pathogenic bacteria on their apical surface. *Proc. Natl. Acad. Sci. U. S. A.* **1995**, *92* (7), 3019.

(20) Barasch, J.; Kiss, B.; Prince, A.; Saiman, L.; Gruenert, D.; Al-Awqati, Q. Defective acidification of intracellular organelles in cystic fibrosis. *Nature* **1991**, *352* (6330), 70–73.

(21) Saiman, L.; Prince, A. *Pseudomonas aeruginosa* pili bind to asialoGM1 which is increased on the surface of cystic fibrosis epithelial cells. *J. Clin. Invest.* **1993**, *92* (4), 1875–1880.

(22) Gellatly, S. L.; Hancock, R. E. W. *Pseudomonas aeruginosa*: new insights into pathogenesis and host defenses. *Pathog. Dis.* **2013**, *67* (3), 159–173.

(23) Lundquist, J. J.; Toone, E. J. The Cluster Glycoside Effect. *Chem. Rev.* **2002**, *102* (2), 555–578.

(24) Leslie, K. G.; Jolliffe, K. A.; Müllner, M.; New, E. J.; Turnbull, W. B.; Fascione, M. A.; Friman, V.-P.; Mahon, C. S. A Glycopolymers Sensor Array That Differentiates Lectins and Bacteria. *Biomacromolecules* **2024**, *25* (11), 7466–7474.

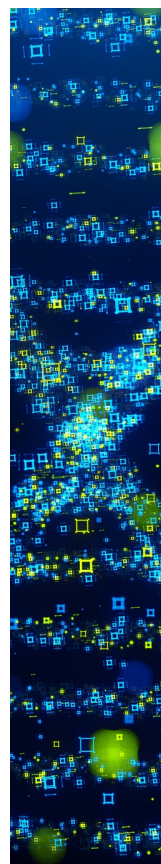
(25) Stewart, S.; Ivy, M. A.; Anslyn, E. V. The use of principal component analysis and discriminant analysis in differential sensing routines. *Chem. Soc. Rev.* **2014**, *43* (1), 70–84.

(26) Geng, Y.; Peveler, W. J.; Rotello, V. M. Array-based “Chemical Nose” Sensing in Diagnostics and Drug Discovery. *Angew. Chem., Int. Ed.* **2019**, *58* (16), 5190–5200.

(27) Mitchell, L.; New, E. J.; Mahon, C. S. Macromolecular Optical Sensor Arrays. *ACS Appl. Polym. Mater.* **2021**, *3* (2), 506–530.

(28) Li, Z.; Askim, J. R.; Suslick, K. S. The Optoelectronic Nose: Colorimetric and Fluorometric Sensor Arrays. *Chem. Rev.* **2019**, *119* (1), 231–292.

- (29) Anzenbacher, P.; Lubal, P.; Buček, P.; Palacios, M. A.; Kozelkova, M. E. A practical approach to optical cross-reactive sensor arrays. *Chem. Soc. Rev.* **2010**, *39* (10), 3954–3979.
- (30) Basu Roy, S.; Nabawy, A.; Chattopadhyay, A. N.; Geng, Y.; Makabenta, J. M.; Gupta, A.; Rotello, V. M. A Polymer-Based Multichannel Sensor for Rapid Cell-Based Screening of Antibiotic Mechanisms and Resistance Development. *ACS Appl. Mater. Interfaces* **2022**, *14* (23), 27515–27522.
- (31) Held, K.; Ramage, E.; Jacobs, M.; Gallagher, L.; Manoil, C. Sequence-Verified Two-Allele Transposon Mutant Library for *Pseudomonas aeruginosa* PAO1. *J. Bacteriol.* **2012**, *194* (23), 6387–6389.
- (32) Chemani, C.; Imberty, A.; de Bentzmann, S.; Pierre, M.; Wimmerová, M.; Guery, B. P.; Faure, K. Role of LecA and LecB Lectins in *Pseudomonas aeruginosa*-Induced Lung Injury and Effect of Carbohydrate Ligands. *Infect. Immun.* **2009**, *77* (5), 2065–2075.
- (33) Huang, B.; Whitchurch, C. B.; Mattick, J. S. FimX, a multidomain protein connecting environmental signals to twitching motility in *Pseudomonas aeruginosa*. *J. Bacteriol.* **2003**, *185* (24), 7068–7076.
- (34) Remminghorst, U.; Rehm, B. H. A. Alg44, a unique protein required for alginate biosynthesis in *Pseudomonas aeruginosa*. *FEBS Lett.* **2006**, *580* (16), 3883–3888.
- (35) Xuan, G.; Lin, H.; Li, X.; Kong, J.; Wang, J. RetS Regulates Phage Infection in *Pseudomonas aeruginosa* via Modulating the GacS/GacA Two-Component System. *J. Virol.* **2022**, *96* (8), No. e0019722.
- (36) Ventre, I.; Goodman, A. L.; Vallet-Gely, I.; Vasseur, P.; Soccia, C.; Molin, S.; Blevès, S.; Lazdunski, A.; Lory, S.; Filloux, A. Multiple sensors control reciprocal expression of *Pseudomonas aeruginosa* regulatory RNA and virulence genes. *Proc. Natl. Acad. Sci. U. S. A.* **2006**, *103* (1), 171–176.
- (37) Duke, R. M.; Veale, E. B.; Pfeffer, F. M.; Kruger, P. E.; Gunnlaugsson, T. Colorimetric and fluorescent anion sensors: an overview of recent developments in the use of 1,8-naphthalimide-based chemosensors. *Chem. Soc. Rev.* **2010**, *39* (10), 3936–3953.
- (38) Leslie, K. G.; Jacquemin, D.; New, E. J.; Jolliffe, K. A. Expanding the Breadth of 4-Amino-1,8-naphthalimide Photophysical Properties through Substitution of the Naphthalimide Core. *Chem. Eur. J.* **2018**, *24* (21), 5569–5573.
- (39) Dougherty, G. *Pattern Recognition and Classification: an Introduction*; Springer: New York, 2013.
- (40) Anderson, M. J. Permutational Multivariate Analysis of Variance (PERMANOVA). *Wiley Statsref: Statistics Reference Online* John Wiley & Sons, Ltd. Hoboken, NJ 2017:1–15.
- (41) Palacios, M. A.; Wang, Z.; Montes, V. A.; Zyryanov, G. V.; Anzenbacher, P. Rational Design of a Minimal Size Sensor Array for Metal Ion Detection. *J. Am. Chem. Soc.* **2008**, *130* (31), 10307–10314.
- (42) Varki, A.; Gagneux, P. Multifarious roles of sialic acids in immunity. *Ann. N. Y. Acad. Sci.* **2012**, *1253* (1), 16–36.
- (43) Marvig, R. L.; Sommer, L. M.; Molin, S.; Johansen, H. K. Convergent evolution and adaptation of *Pseudomonas aeruginosa* within patients with cystic fibrosis. *Nat. Genet.* **2015**, *47* (1), 57–64.
- (44) Tammam, S.; Sampaleanu, L. M.; Koo, J.; Manoharan, K.; Daubaras, M.; Burrows, L. L.; Howell, P. L. PilMNOQP from the *Pseudomonas aeruginosa* type IV pilus system form a transenvelope protein interaction network that interacts with PilA. *J. Bacteriol.* **2013**, *195* (10), 2126–2135.
- (45) Myszka, K.; Czarczyk, K. Characterization of Adhesive Exopolysaccharide (EPS) Produced by *Pseudomonas aeruginosa* Under Starvation Conditions. *Curr. Microbiol.* **2009**, *58* (6), 541–546.
- (46) Filkins, L. M.; O'Toole, G. A. Cystic Fibrosis Lung Infections: Polymicrobial, Complex, and Hard to Treat. *PLoS Pathog.* **2015**, *11* (12), No. e1005258.
- (47) Bottery, M. J.; Johansen, H. K.; Pitchford, J. W.; Friman, V.-P. Co-occurring microflora and mucin drive *Pseudomonas aeruginosa* diversification and pathoadaptation. *ISME Commun.* **2024**, *4* (1), ycae043.
- (48) Bhagirath, A. Y.; Li, Y.; Somayajula, D.; Dadashi, M.; Badr, S.; Duan, K. Cystic fibrosis lung environment and *Pseudomonas aeruginosa* infection. *BMC Pulm. Med.* **2016**, *16* (1), 174.
- (49) Goss, C. H.; Muhlebach, M. S. Staphylococcus aureus and MRSA in cystic fibrosis. *J. Cyst. Fibros.* **2011**, *10* (5), 298–306.
- (50) Dalbøge, C. S.; Hansen, C. R.; Pressler, T.; Hoiby, N.; Johansen, H. K. Chronic pulmonary infection with *Stenotrophomonas maltophilia* and lung function in patients with cystic fibrosis. *J. Cyst. Fibros.* **2011**, *10* (5), 318–325.
- (51) Bottery, M. J.; Matthews, J. L.; Wood, A. J.; Johansen, H. K.; Pitchford, J. W.; Friman, V.-P. Inter-species interactions alter antibiotic efficacy in bacterial communities. *ISME J.* **2022**, *16* (3), 812–821.
- (52) Burdge, D. R.; Noble, M. A.; Campbell, M. E.; Krell, V. L.; Speert, D. P. *Xanthomonas maltophilia* Misidentified as *Pseudomonas cepacia* in Cultures of Sputum from Patients with Cystic Fibrosis: A Diagnostic Pitfall with Major Clinical Implications. *Clin. Infect. Dis.* **1995**, *20* (2), 445–448.
- (53) European Centre for Disease Prevention and Control. *Healthcare-associated infections acquired in intensive care units - Annual Epidemiological Report for 2020*; European Centre for Disease Prevention and Control, 2024.



CAS BIOFINDER DISCOVERY PLATFORM™

STOP DIGGING THROUGH DATA —START MAKING DISCOVERIES

CAS BioFinder helps you find the
right biological insights in seconds

Start your search

